Journal of the European Ceramic Society 21 (2001) 2593–2598

www.elsevier.com/locate/jeurceramsoc

Effects of variations in crystal structure on microwave dielectric properties of Y_2BaCuO_5 system

Akinori Kan[a,*], Hirokata Ogawa[a], Hitoshi Ohsato[b], Soichi Ishihara[a]

[a]*Faculty of Science and Technology, Meijo University, 1-501 Shiogamaguchi, Tenpaku-ku, Nagoya 468-8502, Japan*
[b]*Department of Material Science and Engineering, Nagoya Institute of Technology, Gokiso-cho, Showa-ku, Nagoya 466-8555, Japan*

Abstract

The dielectric properties of $(Y_{2-x}R_x)BaCuO_5$ (R = Sm, Gd, Dy, Ho, Er and Tm) solid solutions were measured for the application as a new microwave resonator. Moreover, the relationships between the results of the dielectric properties obtained and variation in the crystal structure of $(Y_{2-x}R_x)BaCuO_5$ solid solutions have been studied in some detail using the results of Reitveld analysis. The result is that ε_r changes from 12.7 to 19.6 and depend on the ionic radii of the rare-earth which composed the R_2O_{11} polyhedron. Then, τ_f was largely improved by substituting R for Y, and in the case of Dy_2BaCuO_5 compound, the value was −6.4ppm/°C. Using the results of Rietveld analysis obtained at 20 and 80°C, negative values of τ_ε were considered to be caused by a decrease in the atomic distances of the R_2O_{11} polyhedron in the direction of the b-axis. As for the $Q{\cdot}f$ value, it suggests that the difference of $Q{\cdot}f$ value between $x=1$ and 2 is reduced by the strain of R_2O_{11} polyhedron which is caused by the difference of ionic radii of Y and R.

Keywords: Green phase; Microwave resonator; Rare-earth; Rietveld analysis; R_2BaCuO_5

1. Introduction

The Y_2BaCuO_5 compound, the so-called "green phase", is well known as an insulator phase of $YBa_2Cu_3O_{7-x}$ high-temperature superconductors, and is also reported as a new material for a microwave dielectric resonator.[1] Kosky et al.[2,3] reported the dielectric properties of $RBa_2SnO_{5.5}$ (R= rare-earth) substrates for YBCO and BPSCCO superconductor films. The crystal structure of Y_2BaCuO_5 compound was reported by Michel and Raveau,[4] using X-ray powder diffraction, and is an orthorhombic with space group *Pnma* (No. 62). Also, as regards the thermodynamics approach, Roth et al.[5] reported the equilibrium phase diagram of $BaO{:}5(1/2Y_2O_3)$–$3BaO{:}5CuO$ in the system BaO–$1/2(Y_2O_3)$–CuO. In the phase diagram, it was clarified that Y_2BaCuO_5 decomposes into Y_2O_3 and a liquid phase at around 1280 °C.

The detail on the microwave dielectric properties of $Y_2Ba(Cu_{1-x}Zn_x)O_5$ solid solutions were investigated in our previous work.[6] The results have shown that the ε_r values range from 13 to 15, and then τ_f and $Q{\cdot}f$ values range from −38 to −43 (ppm/°C) and from 2×10^4 to 1.1×10^5 (GHz), respectively. Moreover, it was clarified that the substitution of Zn for Cu in Y_2BaCuO_5 solid solutions greatly improves the $Q{\cdot}f$ value, whereas it does not τ_f. We speculate that the substitution for another site, especially the Y site, may be effective in improving τ_f. Therefore, the microwave dielectric properties by rare-earth substitution for Y in Y_2BaCuO_5 compounds were studied in this work, and then the crystal structure of $(Y_{2-x}R_x)BaCuO_5$ solid solution was refined to elucidate the relationship between the microwave dielectric properties and the variation in the atomic distances and angles, using the Rietveld method.[7]

2. Experimental

$(Y_{2-x}R_x)BaCuO_5$ solid solutions were prepared by the solid-state reaction method. High-purity Y_2O_3(99.9%), R_2O_3(99.9%) (R = Sm, Gd, Dy, Ho, Er, Tm and Yb), $BaCO_3$(99.9%) and CuO(99.9%) were weighed based on stoichiometry into $(Y_{2-x}R_x)BaCuO_5$ solid solutions. The powders were mixed with acetone and calcined in an alumina crucible at 950 °C for 20 h in air.

* Corresponding author. Tel.: +81-52-832-1151; fax: +81-52-832-1253.
E-mail address: d3013001@meijo-u.ac.jp (A. Kan).

0955-2219/01/$ - see front matter
PII: S0955-2219(01)00322-3

The calcined powders ground with an organic binder were passed through a screen mesh and pressed into a pellet 12 mm in diameter and 7 mm thick under the cold isotropic pressure (CIP) of 300 MPa. The pellets obtained by the process were sintered for 2 h in air under the sintering temperatures of the samples which were determined by differential thermal analysis (DTA) and thermogravimetry (TG). The sintered pellets were polished and annealed at 900 °C in order to remove any strain. Then, $(Y_{2-x}R_x)BaCuO_5$ solid solutions were ground and mixed with a calibration standard (Si) prior to insertion into the diffractometer. The lattice parameters were determined by the least-squares method. The powder X-ray diffraction (XRPD) data for Rietveld analysis were obtained by step scanning over the angular range (2θ) from 10 to 90°, in increments of 0.03° and a counting time of 3.0 s per step. Then, the variations in the crystal structure *R*-substituted for Y at room temperature are clarified by refining R_2BaCuO_5 solid solutions for $R=$ Dy, Tm, Er using the Rietveld analysis program "RIETAN".[8] Then, the refinements were performed using the initial values of positional parameters for Y_2BaCuO_5 compound reported by Michel and Raveau.[4] Moreover, in order to evaluate the relationship between the temperature coefficient of the resonant frequency and variation in the crystal structure, the XRPD patterns of R_2BaCuO_5 solid solution were obtained at 80 °C, which was the measurement temperature of τ_f. The dielectric properties of R_2BaCuO_5 solid solutions were measured according to Hakki and Coleman's method.[9]

3. Results and discussion

The crystal structure of $(Y_{2-x}R_x)BaCuO_5$ ($R=$Sm, Gd, Dy, Ho, Er, Tm and Yb) solid solutions which belong to orthorhombic is shown in Fig. 1. The crystal structure of the solid solutions is expressed by the three polyhedra such as CuO_5 pyramid at which Cu^{2+} ion is located at the bottom of the pyramid, R_2O_{11} and BaO_{11} polyhedra. In this case, R^{3+} ions are surrounded by seven oxygen atoms and these atoms compose the $R(1)O_7$ and $R(2)O_7$ capped prisms. Then, these prisms are linked each other with common faces into R_2O_{11} polyhedron. Moreover, Ba^{2+} ions are surrounded by 11 oxygen atoms in order to compose the BaO_{11} polyhedron structure.

All $(Y_{2-x}R_x)BaCuO_5$ solid solutions are recognized to form the single phase at $x=1$ and 2 from the results of XRPD analysis. Fig. 2 shows the lattice parameters of $(Y_{2-x}R_x)BaCuO_5$ solid solutions at $x=$ 1 and 2 as a function of ionic radii of rare-earth elements. At both composition $x=1$ and 2, it is recognized that the lattice parameters are increased linearly with increasing the ionic radii of rare-earth elements. Then, the ratio of the variations in the lattice parameters at $x=2$ are larger than those at $x=1$ as shown in Fig. 2. These tendencies are considered to be caused by the occupations of the rare-earth at both *R*(1) and *R*(2) sites. In addition, the lattice parameters of the solid solutions, at which the ionic radii of rare-earth are larger than that of Ho, are

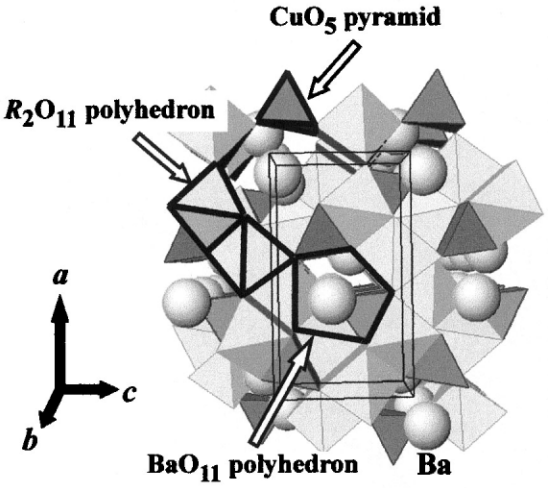

Fig. 1. Crystal structure of $(Y_{2-x}R_x)BaCuO_5$ solid solutions along the *b*-axis.

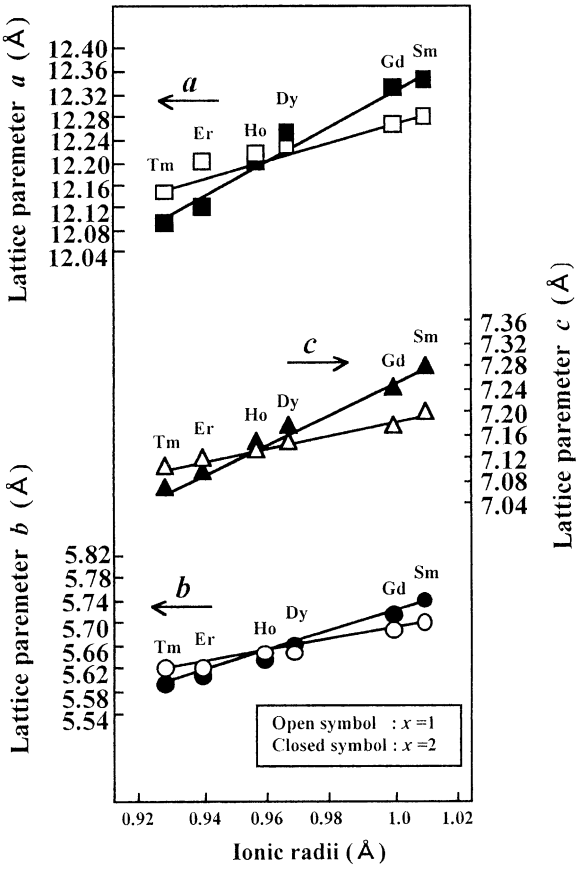

Fig. 2. Lattice parameters of $(Y_{2-x}R_x)BaCuO_5$ solid solutions as a function of the ionic radii for rare-earth.

increased in comparison with those of Y_2BaCuO_5 compound. On the other hand, the lattice parameters of the solid solutions which ionic radii are smaller than Ho are decreased in comparison with those of Y_2BaCuO_5 compound. Also, the lattice parameters of $(Y_{2-x}Ho_x)BaCuO_5$ solid solutions at $x=1$ and 2 have not indicated the remarkable differences compared with those of Y_2BaCuO_5 compound, because the ionic radius of Ho closes to that of Y. Therefore, it suggests that the lattice parameters of this crystal structure especially depend on the differences of the ionic radii for the rare-earth elements. Moreover, in this study, all the $(Y_{2-x}R_x)BaCuO_5$ solid solutions satisfy the Vegard's law which confirms the formation of the solid solutions because the lattice parameters change linearly throughout the entire composition range.

Fig. 3 shows the refined XRPD patterns for Er_2BaCuO_5 compound at 20 and 80 °C, using the Rietveld method. The solid line represents the calculated intensities, whereas the solid squires represent the observed intensities. Moreover, the short virtual bars mean the Bragg's reflection positions and the delta show the differences of intensities between the calculated and observed intensities. The refined atomic coordinates of R_2BaCuO_5 solid solutions for $R=$Dy, Er and Tm obtained at 20 and 80 °C are shown in Table 1. These atomic coordinates of the solid solutions at 20 °C shows the similar results which are reported by Salinas-Sanchez et al.[10] Based on these atomic coordinates as listed in Table 1 the atomic distances and bond angles of CuO_5 pyramid and R_2O_{11} polyhedron were determined.

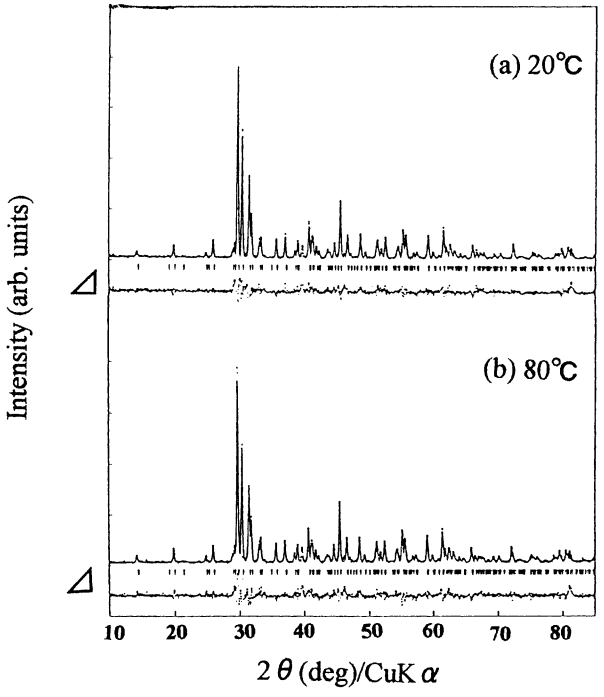

Fig. 3. Refined XRPD patterns of Er_2BaCuO_5 compound at 20 and 80 °C.

The atomic distances and angles of CuO_5 pyramid in the samples for $R=$Dy, Er and Tm maintained at 20–80 °C are listed in Table 2. The bond angles in the CuO_5 pyramid do not so change in the temperature range 20–80 °C whereas the atomic distances obtained at 80 °C are larger than those obtained at 20 °C. Namely, the atomic distances, O1–O1 and O2-O2, which are parallel in the direction of the *b*-axis, change largely as shown in Table 2. On the other hand, the atomic distances O1–O2 and Cu–O3, which are approximately parallel in the direction of *a*-axis and *c*-axis, do not change with increasing temperature because the Ba ion which has the

Table 1
Refined atomic coordinates of R_2BaCuO_5 for $R=$Tm, Er and Dy at 20 and 80 °C

Atoms	Sites	*g*	*x*	*y*	*z*
20 °C					
Tm(1)	4(*c*)	1.0	0.2898(2)	0.25	0.1172(1)
Tm(2)	4(*c*)	1.0	0.0742(1)	0.25	0.3979(7)
Ba	4(*c*)	1.0	0.9035(4)	0.25	0.9288(8)
Cu	4(*c*)	1.0	0.6559(9)	0.25	0.7158(8)
O(1)	8(*d*)	1.0	0.4075(9)	0.0072(6)	0.1675(2)
O(2)	8(*d*)	1.0	0.2200(5)	0.5119(1)	0.3519(1)
O(3)	4(*c*)	1.0	0.1010(7)	0.25	0.0786(1)
Er(1)	4(*c*)	1.0	0.2897(3)	0.25	0.1162(7)
Er(2)	4(*c*)	1.0	0.0735(3)	0.25	0.3979(6)
Ba	4(*c*)	1.0	0.9036(3)	0.25	0.9287(7)
Cu	4(*c*)	1.0	0.6573(1)	0.25	0.7170(8)
O(1)	8(*d*)	1.0	0.4133(1)	0.0042(1)	0.1692(1)
O(2)	8(*d*)	1.0	0.2304(4)	0.5038(7)	0.3437(1)
O(3)	4(*c*)	1.0	0.0979(1)	0.25	0.0730(1)
Dy(1)	4(*c*)	1.0	0.2896(4)	0.25	0.1161(8)
Dy(2)	4(*c*)	1.0	0.0731(4)	0.25	0.3972(7)
Ba	4(*c*)	1.0	0.9040(4)	0.25	0.9290(7)
Cu	8(*d*)	1.0	0.6617(3)	0.25	0.7179(9)
O(1)	4(*c*)	1.0	0.4266(8)	0.0043(5)	0.1703(7)
O(2)	8(*d*)	1.0	0.2353(5)	0.5037(9)	0.3342(1)
O(3)	4(*c*)	1.0	0.0986(5)	0.25	0.0653(5)
80 °C					
Tm(1)	4(*c*)	1.0	0.2890(7)	0.25	0.1189(5)
Tm(2)	4(*c*)	1.0	0.0741(7)	0.25	0.3976(3)
Ba	4(*c*)	1.0	0.9042(8)	0.25	0.9303(5)
Cu	4(*c*)	1.0	0.6574(8)	0.25	0.7151(4)
O(1)	8(*d*)	1.0	0.4120(1)	0.0001(5)	0.1700(3)
O(2)	8(*d*)	1.0	0.2046(5)	0.4888(7)	0.3542(5)
O(3)	4(*c*)	1.0	0.0983(5)	0.25	0.0730(1)
Er(1)	4(*c*)	1.0	0.2887(6)	0.25	0.1164(2)
Er(2)	4(*c*)	1.0	0.0730(6)	0.25	0.3973(5)
Ba	4(*c*)	1.0	0.9040(6)	0.25	0.9281(1)
Cu	4(*c*)	1.0	0.6592(5)	0.25	0.7160(7)
O(1)	8(*d*)	1.0	0.4166(1)	0.0063(1)	0.1685(2)
O(2)	8(*d*)	1.0	0.2197(5)	0.5004(4)	0.3371(9)
O(3)	4(*c*)	1.0	0.0916(1)	0.25	0.0609(1)
Dy(1)	4(*c*)	1.0	0.2889(4)	0.25	0.1158(9)
Dy(2)	4(*c*)	1.0	0.0741(5)	0.25	0.3961(8)
Ba	4(*c*)	1.0	0.9045(5)	0.25	0.9296(1)
Cu	4(*c*)	1.0	0.6594(2)	0.25	0.7150(5)
O(1)	8(*d*)	1.0	0.4357(4)	−0.0044(7)	0.1628(5)
O(2)	8(*d*)	1.0	0.2338(3)	0.5038(4)	0.3352(4)
O(3)	4(*c*)	1.0	0.0995(8)	0.25	0.0683(3)

largest ionic radius in this system suppresses the variations of the atomic distances in these directions. From these variations of the atomic distances in the pyramid, it is recognized that the volume in the CuO_5 pyramid increase with an increase in temperature. The atomic distances of R_2O_{11} polyhedron as listed in Table 3 are decreased with increasing the temperature. These decrements of the atomic distance in the R_2O_{11} polyhedron are considered to be caused by the expansion of the O1–O1 and O2–O2 which are atomic distances inside the CuO_5 pyramid in the direction of the *b*-axis. From the results, the volume in the R_2O_{11} polyhedron is decreased as the temperature is increased in the temperature range 20–80 °C.

Table 4 shows the dielectric properties of $(Y_{2-x}R_x)BaCuO_5$ solid solutions. The resonant frequencies of the solid solutions are ranging from 9.0 to 11.0 GHz, and the relative densities of the samples ranging from 83 to 94%. Then, the dielectric constants of the solid solutions at $x=1$ and 2 are changing from 12.7 to 19.6, and these dielectric constants as a function of ionic radii for rare-earth are shown in Fig. 4. At both composition $x=1$ and 2, the increments of dielectric constants are recognized as the ionic radii of rare-earth are increased. In addition, the dielectric constants at $x=2$ are larger than those at $x=1$. Thus, from these results, the increment of dielectric constants at both composition $x=1$ and 2 are considered to be caused by the difference of the ionic radii for rare-earth, which induce the changes of unit cell volume and the variation in the volume of R_2O_{11} polyhedron. In addition, the difference of dielectric constants between $x=1$ to 2 are caused according to the strain of R_2O_{11} polyhedron induced by the differences of ionic radii between Y and *R* ions.

The temperature coefficient of resonant frequency are ranging from −35 to −6 ppm/°C, and good values are obtained at Dy_2BaCuO_5 compound. All τ_f values obtained at $x=2$ for $(Y_{2-x}R_x)BaCuO_5$ solid solutions are improved in comparison with those at $x=1$. Therefore, it suggests that the improvements of τ_f as composition *x*

Table 2
Atomic distances and angles of CuO_5 pyrimid

R	Atomic distances (Å) and angles (°)	20 °C	80 °C
Tm	Cu–O(1)	1.835(1)	1.853(3)
	Cu–O(2)	2.068(1)	2.103(2)
	Cu–O(3)	2.187(2)	2.199(5)
	<O(1)CuO(1)	104.16	102.45
	<O(2)CuO(2)	80.75	83.07
	<O(1)CuO(3)	107.54	106.06
	<O(2)CuO(3)	89.95	90.60
Er	Cu-O(1)	1.855(3)	1.903(1)
	Cu-O(2)	1.908(1)	1.902(4)
	Cu-O(3)	2.136(5)	2.134(1)
	<O(1)CuO(1)	102.14	99.99
	<O(2)CuO(2)	87.69	85.77
	<O(1)CuO(3)	101.45	102.21
	<O(2)CuO(3)	92.61	95.98
Dy	Cu-O(1)	1.954(6)	2.051(3)
	CuO(2)	1.940(1)	1.946(2)
	Cu-O(3)	2.155(1)	2.156(1)
	<O(1)CuO(1)	95.34	89.59
	<O(2)CuO(2)	92.27	91.92
	<O(1)CuO(3)	101.62	102.01
	<O(2)CuO(3)	92.69	93.07

Table 3
Atomic distances of R_2O_{11} polyhedron

R	Atomic distance (A)	20 °C	80 °C
Tm	Tm(1)—O(1)	2.005(2)	2.036(3)
	Tm(1)—O(2)	2.376(1)	2.338(1)
	Tm(1)—O(2)	2.310(2)	2.349(1)
	Tm(1)—O(3)	2.301(1)	2.326(5)
	Tm(2)—O(1)	2.480(2)	2.459(4)
	Tm(2)—O(1)	2.404(5)	2.403(1)
	Tm(2)—O(2)	2.322(2)	2.277(2)
	Tm(2)—O(3)	2.283(2)	2.279(5)
Er	Er(1)—O(1)	2.107(2)	2.108(2)
	Er(1)—O(2)	2.366(3)	2.437(2)
	Er(1)—O(2)	2.302(1)	2.273(4)
	Er(1)—O(3)	2.426(2)	2.426(1)
	Er(2)—O(1)	2.408(2)	2.392(2)
	Er(2)—O(1)	2.471(4)	2.471(3)
	Er(2)—O(2)	2.502(1)	2.315(3)
	Er(2)—O(3)	2.380(3)	2.403(1)
Dy	Dy(1)—O(1)	2.214(1)	2.298(2)
	Dy(1)—O(2)	2.224(2)	2.236(1)
	Dy(1)—O(2)	2.473(3)	2.467(3)
	Dy(1)—O(3)	2.362(4)	2.341(2)
	Dy(2)—O(1)	2.321(2)	2.234(3)
	Dy(2)—O(1)	2.430(1)	2.397(3)
	Dy(2)—O(2)	2.492(3)	2.467(1)
	Dy(2)—O(3)	2.394(2)	2.367(1)

Table 4
Dielectric properties of $(Y_{2-x}R_x)BaCuO_5$ solid solutions

R	*x*	D_r (%)	*d* (mm)	*h* (mm)	*f* (GHz)	ε_r	τ_f (ppm/°C)	$Q{\cdot}f$ (GHz)
Tm	1	88.6	10.583	5.284	11.095	12.7	−27.3	17 889
	2	89.2	10.168	5.036	9.767	12.8	−14.8	14 409
Er	1	85.6	10.334	5.317	10.590	13.3	−34.2	16 054
	2	83.9	10.561	5.218	11.012	13.5	−26.1	12 564
Ho	1	88.7	10.363	5.215	10.714	13.9	−29.8	12 056
	2	90.2	10.225	5.179	10.486	15.3	−19.3	9360
Dy	1	89.4	10.389	5.211	10.739	14.0	−22.1	42 602
	2	93.4	10.214	4.994	10.561	14.9	−6.4	31 617
Gd	1	86.5	10.381	5.263	10.930	14.0	−35.2	14 304
	2	87.1	10.416	5.089	11.056	16.0	−27.7	3324
Sm	1	84.7	10.651	5.200	11.062	12.6	−29.9	25 136
	2	84.1	10.766	4.989	11.363	19.6	−8.7	3397

R, rare-earth element; D_r, relative density, *d*, *h*, dimension of the samples; *f*, resonant frequency; ε_r, dielectric constant; $Q{\cdot}f$, quality factor; τ_f, temperature coefficient of the resonant frequency.

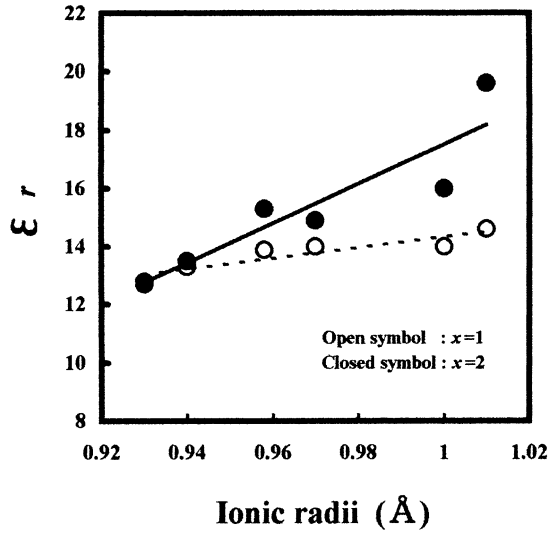

Fig. 4. Dielectric constants of $(Y_{2-x}R_x)BaCuO_5$ solid solutions as a function of the ionic radii for rare-earth.

are increased are caused by the difference of ionic radii between Y and R which induce the strain of R_2O_{11} polyhedron and the variation of crystal structure. Also, at composition $x=2$, the relationships between the crystal structure with increasing the temperature and the temperature coefficient of the resonant frequency are discussed on the basis of the changes in the atomic distances of CuO_5 pyramid and R_2O_{11} polyhedron as shown in Tables 2 and 3, respectively. Generally, τ_f is expressed with the following equation: $\tau_f = -(\tau_\varepsilon/2+\alpha)$. Here, α is the thermal expansion coefficient which determined by the changes in the lattice parameters at 20 and 80 °C. Then, α of $(Y_{2-x}R_x)BaCuO_5$ (R = Dy, Tm and Er) solid solutions are 29.4, 31.6 and 28.9 ppm/°C, respectively. Thus, from these results and τ_f values, the temperature coefficient of the dielectric constant (τ_ε) for R = Dy, Tm and Er are determined by means of the equation as mentioned above. Consequently, τ_ε values for R = Dy, Tm and Er are −46.0, −10.8 and −28.2 ppm/°C, respectively. Since the τ_ε values are negative, these values suggest that the dielectric constant of the solid solutions with an increase in temperature are decreased and the volume of the polyhedron in the unit cell obtained at 80 °C which is related with the τ_ε are decreased in comparison with those at 20 °C. Therefore, it may be account for the variation in the polyhedron with the increase in the temperature of the unit cell, because the change of the polyhedron and τ_ε are interrelated in this crystal structure.

In CuO_5 pyramid, since the increments of the volume in the pyramid with an increase in temperature are recognized as mentioned above, the variation of the CuO_5 pyramid do not coincide with the results of the τ_ε. Moreover, the changes in the volume of the BaO_{11} polyhedron are difficult to relate with the τ_ε, so the variation in the polyhedron do not so change in the temperature range 20–80 °C. However, the changes in the volume of R_2O_{11} polyhedron with increasing the temperature agree with the results of τ_ε, because the volume of the R_2O_{11} with increasing the temperature shows the decrements as described before. Therefore, it is clarified that the change in the volume of R_2O_{11} polyhedron which is induced by the decrement of the atomic distances influence on the τ_ε.

As listed in Table 4, $Q{\cdot}f$ values of $(Y_{2-x}R_x)BaCuO_5$ solid solutions are located from 3300 to 43 000 GHz and maximum value is 42602 GHz at Dy_2BaCuO_5 compound. Comparing the $Q{\cdot}f$ values at both composition $x=1$ and 2, the values at $x=1$ are larger than those at $x=2$. Then, in order to elucidate the effect of the substitution R for Y on the $Q{\cdot}f$ value, $\Delta Q{\cdot}f$ which is the difference between the $Q{\cdot}f$ value at $x=1$ and 2 were determined. Here, $\Delta Q{\cdot}f$ of $(Y_{2-x}R_x)BaCuO_5$ (R = Tm, Er, Ho, Dy, Gd and Sm) solid solutions are 3480, 3490, 2696, 10 985, 10 980 and 21 740 GHz, respectively. From these results, $\Delta Q{\cdot}f$ for $(Y_{2-x}Ho_x)BaCuO_5$ solid solution is smaller than that of any other compound as suggested from the crystal structure of composition $x=1$. In the case of the (YHo)$BaCuO_5$ compound, since the difference of ionic radii for Y and Ho are smaller than other rare-earth ions, the strain of R_2O_{11} polyhedron caused by the difference of the ionic radii does not change. Therefore, it is considered that the strain of the R_2O_{11} polyhedron is induced by the ionic size of rare-earth exerted on the $Q{\cdot}f$ value in the $(Y_{2-x}R_x)BaCuO_5$ solid solutions.

4. Conclusion

$(Y_{2-x}R_x)BaCuO_5$ solid solutions were prepared by the solid-state reaction method, and the formation of the single phase was recognized at both the composition of $x=1$ and 2. From the results of the powder XRD studies, it is clarified that the lattice parameters of the solid solutions are increased as the ionic radii of rare-earth are increased.

The dielectric constants of the solid solutions are ranging from 12.7 to 19.6, and the increments of ε_r are recognized as the ionic radii of rare-earth are increased. Also, τ_f of the solid solutions are ranged from −35 to −6 ppm/°C, and good value is obtained using Dy_2BaCuO_5 compound. In addition, from the results of the Rietveld analysis at 20–80 °C which are the measuring temperature, it suggests that the decrements of the volume in R_2O_{11} polyhedron which are caused by the expansion of the atomic distances, O1–O1 and O2–O2 in the direction of the b-axis with increasing the temperature influence on the τ_ε in this crystal structure. $Q{\cdot}f$ values of the solid solutions are changed from 3300 to 43,000 GHz. Comparing $Q{\cdot}f$ values of composition $x=1$ with those of $x=2$, it is considered that the strain

of the R_2O_{11} polyhedron is induced by the difference of ionic radii Y and R influence on the $Q{\cdot}f$ value.

References

1. Ogawa, H., Watanabe, M., Ohsato, H. and Humphreys, C., Microwave dielectric properties of $(Y_{2-x}R_x)BaCuO_5$ (R = rare-earth) solid solutions. In *Proceeding of the Eleventh IEEE International Symposium on Application of Ferroelectrics*. ISAF, 1998, p. 517.
2. Kosky, J. *et al*, Superconducting Bi-cuprate thick film $T_{c(o)} = 110K$ on $DyBa_2SnO_{5.5}$: a newly developed perovskite substrate. *Appl. Phys. Lett.,* 1994, **65**, 2857–2859.
3. Kosky, J. *et al*, Superconducting YBCO and YBCO–Ag thick films ($T_{c(o)} = 92K$) by dip coating on $GdBa_2HfO_{5.5}$, a new perovskite ceramic substrate. *Superconductor Science and Technology,* 1995, **8**, 525–528.
4. Michel, C. and Raveau, B., Les oxides A_2BaCuO_5 (A = Y, Sm, Eu, Gd, Dy, Ho, Er, Yb). *J. Solid State Chem.,* 1982, **43**, 73.
5. Roth, R. S. *et al*., Phase equilibria and crystal chemistry in the quaternary system Ba–Sr–Y–Cu–O in air. *J. Am. Ceram. Soc*., 1989, **72**, 395–399.
6. Watanabe, M., Ogawa, H., Ohsato, H. and Humphreys, C., Microwave dielectric properties of $Y_2Ba(Cu_{1-x}Zn_x)O_5$ solid solutions. *Jpn. J. Appl. Phys.,* 1998, **37**, 5360.
7. Rietveld, H. M., A profile refinement method for nuclear and magnetic structures. *J. Appl. Crystallogr.,* 1969, **2**, 65.
8. Izumi, F., In *Rietveld Method*, ed. R. A. Young. Oxford University Press, Oxford 1993 (Chapter 13).
9. Hakki, B. W. and Coleman, P. D., A dielectric resonator Method of measuring inductive capacities in the millimeter range. *IRE Trans: Microwave Theory and Technol.,* 1960, **MTT-8**, 402.
10. Salinas-Sanchez, A. *et al*, Structural characterization of R_2BaCuO_5 (R = Y, Lu, Yb, Tm, Er, Ho, Dy, Eu, and Sm) oxides by X-ray and neutron diffraction. *J. Solid State Chem.,* 1992, **100**, 201.